Corresponding Author: Dr. Monica Cristina Gonzalez, PhD.

Corresponding Author's Institution: INIFTA; University of La Plata

First Author: María L Dell'Arciprete

Order of Authors: María L Dell'Arciprete; Juán Soler; Lucas Santos-Juanes; Antonio Arques; Daniel O Mártire; Jorge Furlong; Monica Cristina Gonzalez, PhD.

Abstract: The reaction of three chloronicotinoid insecticides, namely Imidacloprid (IMD), Thiacloprid (THIA) and Acetamiprid (ACT), with carbonate radicals (CO_3^{*-}) was investigated. The second order rate constants $(4 \pm 1) \times 10^6$, $(2.8 \pm 0.5) \times 10^5$, and $(1.5 \pm 1) \times 10^5$ $M^{-1}s^{-1}$ were determined for IMD, THIA and ACT, respectively. The absorption spectra of the organic intermediates formed after CO_3^{*-} attack to IMD is in line with those reported for -aminoalkyl radicals. A reaction mechanism involving an initial charge transfer from the amidine nitrogen of the insecticides to CO_3^{*-} is proposed and further supported by the identified reaction products. The pyridine moiety of the insecticides remains unaffected until nicotinic acid is formed. CO_3^{*-} radical reactivity towards IMD, ACT, and THIA is low compared to that of HO^* radicals, excited triplet states, and $1O_2$, and is therefore little effective in depleting neonicotinoid insecticides.

Waste water specialist

Dear Editor,

Please find enclosed the manuscript entitled: "Removal of neonicotinoid insecticides by carbonate radicals". The present manuscript gives an insight into the reaction mechanisms and kinetics of carbonate radicals with neonicotinoid insecticides, namely imidacloprid, thiacloprid and acetamiprid.

We thank you in advance for your kind cooperation.

Highlights:

Cloronicotinoid insecticides show low reactivity towards carbonate radicals.

The reaction involves an initial charge transfer from the insecticide to $CO_3^{\bullet-}$.

After prolonged irradiation chloronicotinic acid is formed.

Hydroxyl and sulfate radicals are among the most effective in degrading the insecticides.

1   ***Removal of neonicotinoid insecticides by carbonate radicals.***

2   María Laura Dell'Arciprete[a], Juán M. Soler[b], Lucas Santos-Juanes[c], Antonio Arques[b], Daniel

3   O. Mártire[a], Jorge P. Furlong[d], and Mónica C. Gonzalez*[a]

4   [a] Instituto de Investigaciones Fisicoquímicas Teóricas y Aplicadas (INIFTA), Facultad de

5   Ciencias Exactas, Universidad Nacional de La Plata, Casilla de Correo 16, Sucursal 4,

6   (1900) La Plata, Argentina. E-mail: gonzalez@inifta.unlp.edu.ar.

7   [b]Grupo de Procesos de Oxidación Avanzada, Departamento de Ingeniería Textil y Papelera,

8   Universidad Politécnica de Valencia, Campus de Alcoy, Plaza Ferrandiz y Carbonell s/n,

9   03801 Alcoy, Spain

10   [c] CIESOL, Joint Centre of the University of Almería-CIEMAT, Ctra de Sacramento s/n, 04120

11   Almería, Spain.

12   [d] LADECOR, Departamento de Química, Facultad de Ciencias Exactas, Universidad

13   Nacional de La Plata, Casilla de Correo 16, Sucursal , (1900) La Plata, Argentina.

14   *Corresponding author. Tel.: (+54) 221-425-7430; fax: (+54) 221-425-4642.

15   E-mail address: gonzalez@inifta.unlp.edu.ar (M.C. Gonzalez)

16   **Abstract**

17   The reaction of three chloronicotinoid insecticides, namely Imidacloprid (IMD), Thiacloprid

18   (THIA) and Acetamiprid (ACT), with carbonate radicals ($CO_3^{\bullet-}$) was investigated. The second

19   order rate constants $(4 \pm 1)\times10^6$, $(2.8 \pm 0.5)\times10^5$, and $(1.5 \pm 1)\times10^5$ $M^{-1}s^{-1}$ were determined

20   for IMD, THIA and ACT, respectively. The absorption spectra of the organic intermediates

21   formed after $CO_3^{\bullet-}$ attack to IMD is in line with those reported for α-aminoalkyl radicals. A

22   reaction mechanism involving an initial charge transfer from the amidine nitrogen of the

23   insecticides to $CO_3^{\bullet-}$ is proposed and further supported by the identified reaction products.

24   The pyridine moiety of the insecticides remains unaffected until nicotinic acid is formed.

1

25    $CO_3^{\bullet-}$ radical reactivity towards IMD, ACT, and THIA is low compared to that of $HO^{\bullet}$ radicals,

26   excited triplet states, and $^1O_2$, and is therefore little effective in depleting neonicotinoid
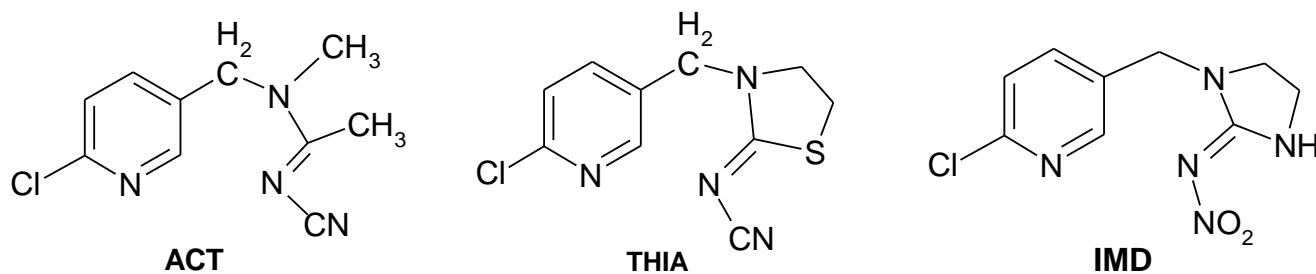
27   insecticides.

28   **Keywords:** carbonate radicals, neonicotinoid insecticides, Imidacloprid, Thiacloprid,

29   Acetamiprid, α-aminoalkyl radical.

30   **1. Introduction**

31   Carbonate radical ($CO_3^{\bullet-}$) is a selective one-electron oxidant, E^0 ($CO_3^{\bullet}/CO_3^{2-}$) = 1.78 V *vs.*

32   NHE, capable of initiating the oxidation of many organic compounds. Carbonate radical

33   reactivity is high for electron rich N-containing chemicals such as heterocycles, fenuron,

34   carbendazim and phenylurea herbicides (Busset *et al.*, 2007, Mazellier *et al.*, 2007). It is also

35   reactive with sulfur-containing compounds such as thioanisole, dibenzothiophene, fenthion,

36   and S-triazine (Canonica *et al.*,2005; Mazellier *et al.*, 2002; Huang and Mabury, 2000b) with

37   reaction rate constants k ranging from 10^6 to 10^8 M^{-1} s^{-1}. Aliphatic alcohols are among the

38   least reactive with k in the range from 10^3 to 10^5 M^{-1} s^{-1} (Clifton and Huie, 1993; Neta *et al.*,

39   1988).

40   Carbonate radicals in natural waters are mainly formed by the reactions of carbonate

41   /bicarbonate ions with either hydroxyl radicals or aromatic-ketones triplet excited states as

42   those contained in dissolved organic matter, DOM (Canonica *et al.*, 2005; Huang and

43   Mabury,2000; Lam *et al.*, 2003; Vione 2009, Wu and Linden, 2010). The steady state

44   concentration of 10^{-13}-10^{-15} M found in natural waters supports the increasing evidence

45   reported in the literature for their important role in the self-cleaning of the hydrosphere

46   basins. Mazellier and coworkers suggested that the degradation of the fungicide

47   carbendazim by $CO_3^{\bullet-}$ in natural waters and carbonate-contaminated effluents cannot be

48   neglected compared to that initiated by hydroxyl radicals [Mazellier *et al.*, 2002]. Also, Huang

49   and Mabury confirmed that $CO_3^{\bullet-}$ contribute to the photodegradation of sulfur-containing

50   xenobiotics in natural and artificial waters [Huang and Mabury, 2000a]. Despite the long

2

51 regarded importance of $CO_3^{\bullet-}$ in the water environment, studies discussing its reaction

52 mechanisms towards organic contaminants are scarce.

53 Neonicotinoid insecticides are among the most important commercial insecticides used

54 worldwide owing to their high insecticidal activity, broad insecticidal spectra, good systemic

55 properties, and suitable field stability [Zabar *et al.*, 2011]. Their photodegradation in aquatic

56 media [Moza *et al.*, 1998; Redlich, *et al.*, 2007; Wamhoff and Schneider, 1999], and in

57 advanced oxidation procedures technologies such as solar photo-Fenton and TiO_2

58 photocatalysis have been reported in the literature [Malato *et al.*, 2001, Cernigoj *et al.*, 2007].

59 In the last years, the reactivity, mechanisms, and primary degradation products of

60 Imidacloprid (IMD), Thiacloprid (THIA) and Acetamiprid (ACT) (Scheme 1) with hydroxyl

61 radical (Dell´Arciprete *et al.*, 2009], singlet oxygen, and excited triplet states have been

62 investigated (Dell´Arciprete *et al.*, 2010]. Here, kinetic and mechanistic studies on $CO_3^{\bullet-}$

63 oxidation of the insecticides IMD, THIA and ACT are reported, and the importance of these

64 reactions in the self cleansing of natural waters is discussed.

ACT   **THIA**   **IMD**

67 **Scheme 1**. Chemical structures of the insecticides (from left to right) Acetamiprid,

68 Thiacloprid, and Imidacloprid.

69 **2. Materials and methods**

70 *2.1. Chemicals*

71 Imidacloprid, Acetamiprid, and Thiacloprid were obtained from Aldrich and used as received.

72 Sodium peroxodisulphate, NaOH, and $HClO_4$ from Merck, were used without further

73   purification. Distilled water was passed through a Millipore system (>18MΩ cm, < 20 ppb of

74   organic carbon). The pH of the solutions was adjusted to 7.7 ± 0.5 with a HCO_3^-/H_2CO_3

75   buffer by addition of $HClO_4$ and measured with a Consort pH-meter model C832.

76   Carbonate radicals are generated *in situ* by reaction of bi/carbonate ions with sulphate

77   radicals. Photolysis of aqueous solutions of $S_2O_8^{2-}$ with excitation wavelengths λ_{exc}< 300

78   nm, reaction (1) in Table 1, is a clean source of sulphate radical ions, $SO_4^{\bullet-}$. The latter

79   radicals are scavenged by excess Na_2CO_3, reaction (2), with rate constant k_2= 3×10^6 $M^{-1}s^{-1}$

80   (Huie, 1991]. Carbonate radicals are expected to be the main oxidizing species in solution if

81     $[CO_3^{2-}]$ ~ 1 M and [insecticides] < 10^{-4} M.

82   2.2. *Time resolved experiments*

83   Flash-photolysis experiments were carried out using a conventional flash apparatus, Xenon

84   Co. model 720C with modified optics and electronics. Two collinear quartz Xenon high-

85   intensity pulsed flash tubes, Xenon Corp. P/N 890-1128 (FWHM $\leq$ 20 μs), with a continuous

86   spectral distribution ranging from 200 to 600 nm and maximum around 450 nm were used.

87   The analysis source was a high pressure mercury lamp (Osram HBO-100 W). The optical

88   path length of the 1 cm internal diameter quartz sample cell was 10 cm. The monochromator

89   collecting the analysis beam (Bausch & Lomb, high intensity) was directly coupled to a

90   photomultiplier (RCA 1P28), which output was fed into a digital oscilloscope (HP 54600B).

91   Digital data were stored in a personal computer. The emission of the flash lamps was filtered

92   with an aqueous concentrated solution of the corresponding insecticide in order to avoid

93   photolysis of the substrate. The temperature (25 ± 3 ^{o}C) was measured inside the reaction

94   cell with a calibrated Digital Celsius Pt-100 Ω thermometer. Freshly prepared solutions were

95   used in order to avoid possible thermal reactions of peroxodisulphate with the substrates.

96   *2.3. Chemical analyses*

97   Samples for product detection were obtained from 254 nm -irradiated oxygen-saturated

98   solutions containing 80 mg/L of the insecticides, 0.025 M of $Na_2S_2O_8$ and 1M of $HNaCO_3$.

99   To that purpose, a 1 liter capacity cylindrical glass reactor continuously bubbled with O_2 was

100   used. The reactor was equipped with an axial immersion lamp Heraeus TNN 15/35 (low

101   pressure Hg covered with commercial quartz), which emits nearly monochromatic radiation

102   at 254 nm. Periodically, samples were taken for analyses. Reaction products were analyzed

103   by GC-MS (GCMS-QP2010S, Shimadzu, equipped with a quadrupole mass analyser). To

104   that purpose, 100 mL of the samples were flown through a LiChrolut EN 200 mg cartridge

105   (Merck). The organics were recovered with 3 mL of methanol and the extracts injected in

106   the GC-MS chromatograph. The GC temperature program increased from 60ºC to 250ºC

107   with a 5ºC/min rate. A Meta X5 Teknokroma column was used. The injection volume was 10

108   μL.

109   Under the experimental conditions used for the detection of products, photolysis of THIA,

110   and ACT is of little significance (< 20 % of the insecticides may be photodegraded at 254 nm

111   after 30 minutes irradiation). On the other hand, despite quantum depletion efficiencies of

112   IMD due to 254 nm photolysis are nine fold times higher those of ACT and THIA, less than

113   35% of the 254 nm light is absorbed by IMD (S.I. Figure 1). Therefore, IMD photolysis is also

114   expected to be of little significance, as supported by the experimental observation that the

115   photolysis products 1-[(6-chloro-3-pyridi-nyl)methyl]-N-nitroso-2-imidazolidinimine and (1-(6-

116   chloro-3-pyridyl-methyl)imidazolidin-2-one) were not among the detected products

117   (Dell´Arciprete *et al.*, 2009).

118   *2.4 Bilinear regression analysis*

119   For each experimental condition, several absorbance decay profiles at different detection

120   wavelengths were taken. Absorbance is thus a function of wavelength and time. Taking

121   advantage of the linearity of the absorbance with both concentrations and absorption

122   coefficients, a bilinear regression analysis was applied to the experimental absorption matrix

123 in order to retrieve information on the minimum number of species and on their relative
124 concentration profiles and absorption spectra (San Román and Gonzalez, 1989].

125 *2.5 Computer simulations:* The kinetic model for computer simulation is based on
126 component balances and equilibrium equations formulated in terms of a differential
127 algebraic equations system which is solved by Gear's Stiff method and a least squares
128 estimation criterion as described elsewhere (Alegre *et al.*,2000, Gear, 1971).

3. Results

3.1. Reactions of $CO_3^{\bullet-}$ radicals with chloronicotinoid insecticides

131 Photolysis of air-saturated solutions of pH 7.7 containing 0.025 M $S_2O_8^{2-}$ and 1 M HCO_3^-
132 showed the formation of a transient species absorbing in the wavelength range from 400 to
133 670 nm whose spectrum taken immediately after the flash of light is in agreement with that
134 reported for $CO_3^{\bullet-}$ (Behar *et al.*, 1970; Busset *et al.*, 2007). Photolysis of the latter solutions
135 in the presence of [insecticides] $< 1 \times 10^{-4}$ M showed absorbance traces in the same
136 wavelength range with decay rates increasing with the insecticide concentration, as shown
137 in Figure 1. The spectrum of the observed transient also agrees with that for $CO_3^{\bullet-}$. The
138 decay of the absorbance traces, A(λ, t), at a given detection wavelength could be well fitted
139 to a mixed first- and second- order decay law given by equation 1.

140
$$A(\lambda,t)=\frac{k_{app}}{b(\lambda)\times exp(a\times t)-c(\lambda)}+d(\lambda) \qquad \text{eq. (1)}$$

141 Where k_{app} is the rate constant for the first order decay, $d(\lambda)$ corresponds to the absorbance
142 of a long living species, $c(\lambda)$ is the second order decay rate constant, $b(\lambda) = (k_{app}/A_0) + c(\lambda)$,
143 and A_0 is the absorbance change immediately after the flash of light.

144 The rate constant for the bimolecular recombination of $CO_3^{\bullet-}$ radicals, reaction 3 in Table 1,
145 may be obtained from the relation c$(\lambda)= 2k_3/\varepsilon l$. Taking c$(\lambda)$ values obtained from the fitting of
146 the traces at 600 nm to eq. (1) and considering $\varepsilon_{600}(CO_3^{\bullet-}) = 2000 \pm 100$ M^{-1} cm^{-1}, it results

147   that $2k_3 = (1.1 \pm 0.1) \times 10^7$ M^{-1} s^{-1} for a reactive mixture of 1.08 ionic strength. The obtained

148   value agrees with that reported for k_3 in solution of ionic strength = 1.5 (Czapski 1994, Zuo

149   and col., 1999). Values of k_{app} obtained from the fitting to eq. (1) are independent of the

150   detection wavelength λ and linearly increase with the analytical concentration of the

151   insecticide, $[Ins]_0$, as shown in Figure 1 *inset* for THIA and ACT. The slope of these straight

152   lines yield the bimolecular rate constants k_4 for reaction (4), depicted in Table 1.

153   Figure 1 about here

154   Table 1 about here

155   The reaction rates obtained for the chloronicotinoid insecticides are on the same order of

156   those reported for the herbicides atrazine (1-chloro-3-ethylamine-5-isopropylamine-2,4,6-

157   tryacine) (Huang and Mabury, 2000b) and fenuron (1,1-dimetyl-3-phenylurea) (Mazellier *et*

158   *al*; 2007), and the fungicide carbendazim (metylbenzimidazol-2-yl-carbamate) (Mazellier *et*

159   *al.*, 2002).

160   To evaluate the possible attack of $CO_3^{\bullet-}$ to the pyridine moiety, kinetic experiments were

161   performed with 3-methylpyridine (3-MePy) and 3-chloropyridine (3-ClPy) as models for the

162   estimation of the reactivity of the pyridine moiety in the insecticides. To these purposes,

163   photolysis of air-saturated 0.025 M $S_2O_8^{2-}$ solutions of pH 7.7 containing 1 M HCO_3^- and

164   pyridine derivatives in concentrations $< 1 \times 10^{-4}$ M, were performed. The rate constants for the

165   reactions of 3-MePy and 3-ClPy with $CO_3^{\bullet-}$ radicals are $k_{3\text{-MePy}} = (3.4 \pm 0.2) \times 10^5$ and $k_{3\text{-ClPy}} =$

166      $(2.2 \pm 0.1) \times 10^4$, respectively. Therefore, a low reactivity of the pyridine moiety of the

167   insecticides with $CO_3^{\bullet-}$ radicals is expected. However, as ACT and THIA also show a low

168   reactivity towards $CO_3^{\bullet-}$, an attack to the pyridine moiety of the pyridines may only be

169   discarded upon an exhaustive product determination. On the other hand, $CO_3^{\bullet-}$ attack on the

170   pyridine moiety of IMD is expected to be of little significance.

171   *3.2 Stable products identification*

7

172 Insecticide degradation products were identified after 15 and 30 minutes continuous UV

173 irradiation (254 nm) of O_2-saturated aqueous solutions of pH 7.7 containing 80 mg/L of the

174 insecticides, 0.025 M of $Na_2S_2O_8$ and 1M of $HNaCO_3$. Table 2 shows the identified products

175 and their mass spectrum (MS).

176   3.3. *Computer simulation of the experiments.*

177 Since $CO_3^{\bullet-}$ radicals are formed from the reaction of the strong oxidizing $SO_4^{\bullet-}$ radicals with

178 excess carbonate ions, there was concern on the possibility that the oxidation of the

179 insecticides could also be initiated by $SO_4^{\bullet-}$, reaction (5), and that the organic radicals thus

180 formed further contribute to the depletion of $CO_3^{\bullet-}$. To probe that such reactions were of little

181 significance under the experimental conditions used for the determination of the rate

182 constants, a computer program was built to simulate the experimental absorbance profiles of

183 $SO_4^{\bullet-}$ and $CO_3^{\bullet-}$. To this purpose, reactions (1) to (5) along with the reactions of $SO_4^{\bullet-}$ with

184 water and peroxodisulphate ions (reactions (6) and (7), respectively), and $SO_4^{\bullet-}$ bimolecular

185 recombination (reaction (8)), were taken into account. The reaction rate constants used are

186 those depicted in Table 1. The flash emission was considered a delta function producing

187 $SO_4^{\bullet-}$ radicals. Initial $SO_4^{\bullet-}$ radical concentration taken as an input parameter, was estimated

188 from experiments under identical conditions but in the absence of carbonate ions, taking ε^{450}

189 $(SO_4^{\bullet-})$ = 1600 M^{-1} cm^{-1} (McElroy, 1990). Only for IMD, a 20 - 30% inner filter effect due to

190 the insecticide absorption of the polychromatic light emitted by the flash lamps was taken

191 into account (see S.I Figure 1). Simulated concentration profiles for these transients were

192 converted into the corresponding absorbance curves and compared to the experimental data

193 to fit the set of experiments. A good agreement between experimental and simulated profiles

194 for $CO_3^{\bullet-}$ traces was observed in the absence and presence of the insecticides, as depicted

195 for IMD by the dotted and dashed lines in Figure 1. Therefore, experimental $CO_3^{\bullet-}$ decay

196 rates give confident information on the k_4 values depicted in Table 1.

197   Since high concentrations of the insecticides were used in the continuous irradiation

198   experiments of section 3.2 to determine the products of reaction (4), the generation of

199   detectable concentrations of products due to the reaction between the insecticides and $SO_4^{\bullet-}$

200   radicals cannot be neglected. In fact, under the experimental conditions used, the relations

201     $k_{5,THIA} \times [THIA]/k_2 \times [CO_3^{2-}] > 0.05$ and $k_{5,ACT} \times [ACT]/k_2 \times [CO_3^{2-}] > 0.05$ apply, strongly suggesting

202   that the competition of THIA (and that of ACT) with CO_3^{2-} anions for $SO_4^{\bullet-}$ radicals is not

203   negligible. To evaluate the magnitude of this contribution, computer simulations were also

204   performed setting as initial parameters the reactant concentrations used in these

205   experiments and considering continuous irradiation conditions. To this purpose, $SO_4^{\bullet-}$

206   radicals were assumed to be formed at a rate of 5×10^{-6} M s^{-1} as expected for the irradiation

207   with a 15 W low-pressure Hg lamp (incident photonic flux at 254 nm = 6.1×10^{-6} E s^{-1}) of a

208   0.025 M $S_2O_8^{-2}$ solution ($S_2O_8^{-2}$ photodissociation quantum yield in the range from 0.5 to 0.7,

209   Criquet *et al*., 2009) contained in a 2.5 cm optical pathway reactor. The stacked bar plot in

210   S. I. Figure 2, shows the percentage of products due to reactions (4) and (5) formed after the

211   quantitative depletion of the insecticides, as retrieved from the computer simulations. From

212   the comparison of the bars it results that the generation of products from reaction (5) is of

213   little significance only for IMD. However, almost 60 and 70 % contribution of the products of

214   reaction (5) is expected for ACT and THIA, respectively.

215   *3.4. Organic radical intermediates.*

216   To obtain information on the nature of the organic transients formed after reaction (4), flash

217   photolysis of argon- or air-saturated solutions of pH 7.7 containing 0.025 M $S_2O_8^{2-}$, 1 M

218   HCO_3^- and 2×10^{-4} M of the insecticides were performed. For each insecticide, several decay

219   profiles were obtained at different wavelengths in the range from 300 to 650 nm. A bilinear

220   regression analysis was applied to each absorbance matrix to gain information on the

221   minimum number of transients formed.

222   *IMD radical intermediates*: For experiments with IMD, the bilinear analysis indicates that the

223   data obtained may be described by two transient species with spectra and decay profiles

9

224 shown in Figure 2. The transient formed immediately after the flash of light shows absorption

225 spectrum coincident with that of $CO_3^{\bullet-}$ (see grey lines in Figure 2, obtained from experiments

226 in the absence of insecticide). The half life of 2 ms observed for this transient is on the order

227 expected for the reaction of $CO_3^{\bullet-}$ with 2×10^{-4} M IMD under the experimental conditions used.

228 The transient formed after the decay of $CO_3^{\bullet-}$ shows an absorption maximum at 300 – 330

229 nm (full circles in Figure 2) and is assigned to the organic transient formed after reaction (4).

230   Figure 2 about here

231 An electron transfer reaction from aminic nitrogen to carbonate radical was proposed for

232 aliphatic amines (Elango *et al.*, 1985), anilines (Elango *et al.*, 1984) and guanine (Shafirovih

233 *et al.*, 2001). Two different mechanisms were proposed for the attack of $CO_3^{\bullet-}$ radicals to

234 aliphatic amines (Elango and co-workers). The electron transfer from the N atom to $CO_3^{\bullet-}$

235 yielding an amine radical cation followed by proton elimination and α-aminoalkyl radical

236 formation seems to be the favored mechanism for tertiary amines. For primary amines, a

237 direct α- hydrogen abstraction to yield an α-aminoalkyl radical seems to take place. Both

238 mechanisms may be competitive in secondary amines. Considering that IMD has a tertiary

239 amine group, the electron transfer mechanism might apply. The electron transfer Gibbs

240 energy from insecticides to $CO_3^{\bullet-}$, $\Delta_{ET}G^0$, can be calculated using equation (2).

241 $$\Delta G_{ET}^{0} = -F \times [E^{0}(CO_3^{\bullet-}/CO_3^{2-}) - E^{0}(Ins^{\bullet+}/Ins)] \qquad \text{eq.(2)}$$

242 Considering $E^{0}(Ins^{\bullet+}/Ins) < 1.2$ V for the reduction potentials of the chloronicotinoid

243 insecticides (Dell'Arciprete *et al.*, 2010) and $E^{0}(CO_3^{\bullet-}/CO_3^{2-}) = 1,78$ V, the value $\Delta_{ET}G^0 < -56$

244 kJ/mol is estimated. Consequently, the electron transfer reactions are thermodynamically

245 allowed and the observed organic transient is suspected to be either an amine radical cation

246 or an α-aminoalkyl radical. As, discussed earlier, $CO_3^{\bullet-}$ radical addition to the pyridine moiety

247 of IMD is of no significance, as also supported by the nature of the observed reaction

248 products which maintain the pyridine ring even after prolonged irradiation.

249 To identify the organic radical formed after reaction (4), the transient spectrum is compared

250 to those obtained by DFT calculations of the IMD radical cation (IMDRC) and α-aminoalkyl

251 radicals published in the literature (Dell Arciprete *et al.*, 2011). The theoretically obtained

252 spectrum of IMDRC evidences an absorption maximum at 300 nm and a less intense band

253 at 410 nm. The α-aminoalkyl radical in the heterocycle (IMDRH) presents an absorption

254 maximum at 310 nm and a shoulder at 450 nm while that of the α-aminoalkyl radical at the

255 methylene bridge (IMDRM) exhibits a maximum around 330 nm. The sum of the spectrum of

256 the two α-aminoalkyl radicals in a 1:1.2 IMDRM: IMDRH ratio shows a good agreement with

257 the organic radical of IMD (see dashed-grey line in Figure 2), and is therefore assigned to

258 these species.

259 *THIA and ACT radical intermediates:* Independent irradiation experiments performed with

260 ACT and THIA show the formation of mainly one transient in the wavelength range from 400

261 to 750 nm with absorption maximum at 600 nm, as shown in Figures S.I.3 and S.I.4 for THIA

262 and ACT, respectively. The transient spectrum is coincident with that of $CO_3^{\bullet-}$ and its ~ 20

263 ms half life is on the order expected for the reaction of $CO_3^{\bullet-}$ with ACT or THIA under the

264 experiment conditions. Therefore, the transient absorbing at $\lambda > 400$ nm is assigned to $CO_3^{\bullet-}$

265 radicals.

266 Due to the slow reaction between $CO_3^{\bullet-}$ and either ACT or THIA, it may be expected that the

267 organic radical intermediates formed from these reactions are present in very low

268 concentrations if their depletion rates are fast. In fact, considering an initial electron transfer

269 from these insecticides to $CO_3^{\bullet-}$, α-aminoalkyl radicals from THIA and ACT are expected to

270 be formed which are reported to decay in the ms time range (Dell´Arciprete *et al.*, 2011). The

271 resolution of the differential mass equations for an intermediate species involved in pseudo-

272 first order consecutive reactions shown in eq. (3), where IR stands for the α-aminoalkyl

273 radicals of either THIA or ACT and k_d is the corresponding intermediate depletion rate

274 constant, leads to equation (4). The subscript "o" indicates initial concentrations taken

275 immediately after the flash of light.

276

$$CO_3^{\bullet-} + \text{Insecticide (excess)} \xrightarrow{k_4} IR \xrightarrow{k_d} \text{Products} \qquad \text{eq. (3)}$$
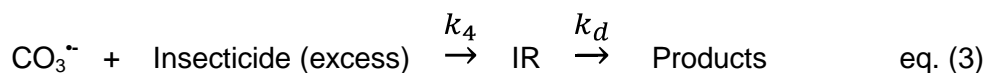
$$[IR] = \left[CO_3^{\bullet-}\right]_0 \frac{k_4 \times [\text{Ins}]}{k_d - k_4 \times [\text{Ins}]} \left[e^{-k_4 \times [\text{Ins}]} - e^{-k_d}\right] \qquad \text{eq. (4)}$$

277

278

279 Under the conditions $k_d > k_4 \times [\text{Ins}]$, the value of k_d is reflected in the short rising portion of the

280 intermediate concentration profile; at longer times, [IR] depletion is dominated by the

281 exponential term $\exp(-k_4 \times [\text{Ins}])$. In fact, the small absorbance traces obtained below 400 nm

282 in experiments with THIA show ~ 1 ms rise time and a 20 ms decay, in agreement with the

283 previous discussion (see Figure S.I.5). Traces obtained at $\lambda > 400$ nm due to $CO_3^{\bullet-}$ show rise

284 times in the μs time range, within the duration of the flash of light. Therefore, the absorption

285 traces obtained in the 350 – 400 nm wavelength range in experiments with THIA may be due

286 to α-aminoalkyl radicals, in coincidence with the reported absorption spectrum for these

287 radicals (Dell'Arciprete *et al.*, 2011).

288   *3.5. Reaction pathways*

289 Based on the detected intermediates and the observed reaction products, a pathway for the

290 primary steps of the $CO_3^{\bullet-}$ oxidation of IMD may be proposed, as shown in Scheme 2. An

291 electron transfer pathway from IMD to $CO_3^{\bullet-}$ yields CO_3^{2-} anions and the radical cation

292 IMDRC (reaction path *a*). Further H^+ elimination from IMDRC leads to the α-aminoalkyl

293 radicals IMDRH, reaction path *b,* and IMDRM, reaction path *c*. The α-aminoalkylradicals are

294 able to reduce O_2 to superoxide (Baciocchi *et al.*, 2004; Hiller and Asmus, 1983; Lalevée *et*

295 *al.*, 2007) and upon further addition of water cleave to yield 6-chloronicotinaldehyde (reaction

296 path *d*). Molecular oxygen addition to IMDRH and the further disproportionation of the

297 resulting peroxyl radical yields the hydroxyl and the keto-derivative of IMD (reaction path *e*).

298 The latter substances were not observed among the identified products; however, product **2**

299 may only be formed from the sequential oxidation of these compounds by $CO_3^{\bullet-}$, reaction

300 path *f*.

301 ***Scheme 2.*** Reaction mechanism of IMD with carbonate radical. The species in brackets are

302 proposed, but not detected.
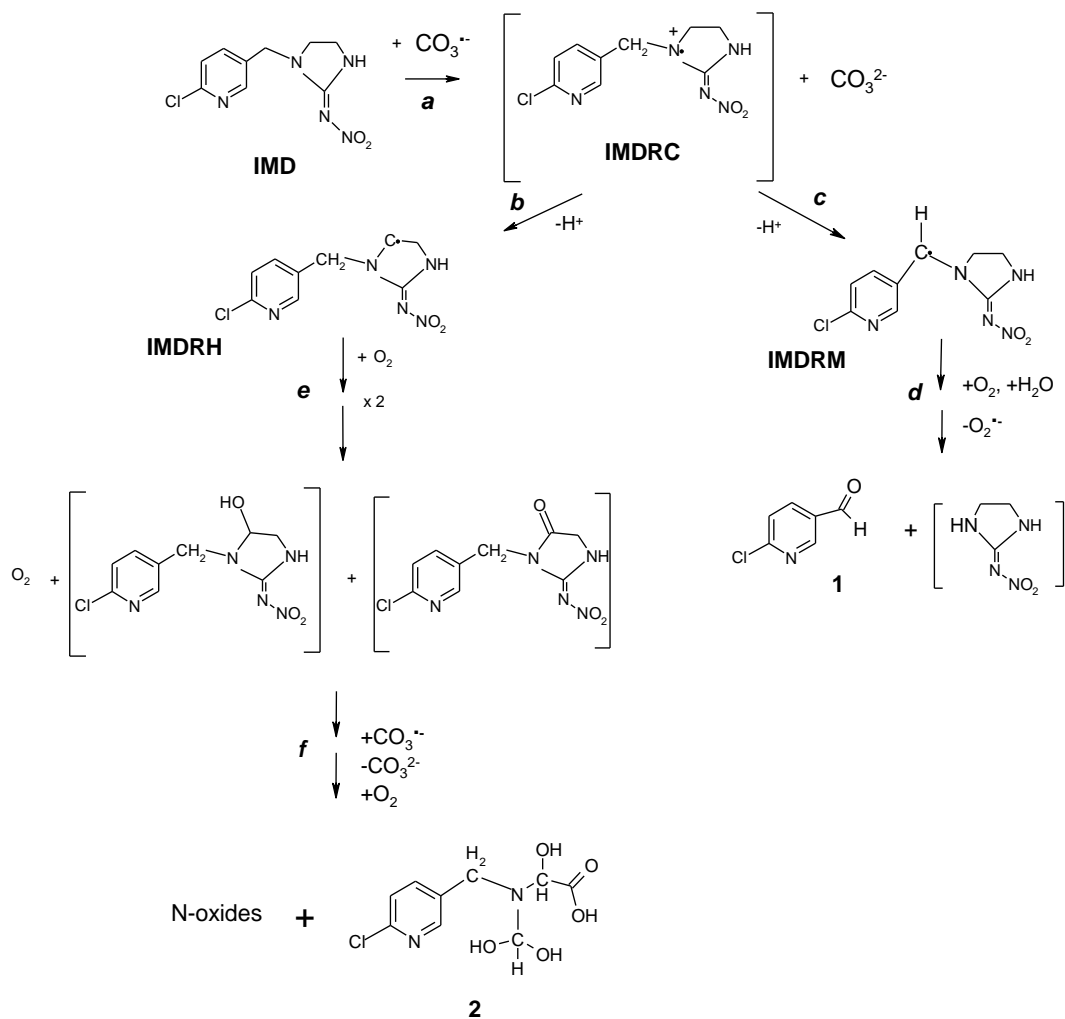
303

304 Formation of THIA α-aminoalkyl radicals and of products **1** and **2** in experiments with THIA

305 may be explained by an initial electron transfer pathway as also suggested for IMD. Briefly,

306 an initial electron transfer from the aminic N of THIA to $CO_3^{\bullet-}$ yields the radical cation of the

307 insecticide, THIARC and CO_3^{2-} anions (reaction path *g* in Scheme 3). Further H^+ elimination

308 at vicinal C leads to the formation of α-aminoalkylradicals in the heterocycle ring, THIARH

309 (reaction path *h*) and from the methylene bridge, THIARM (reaction pathway *i*). Reaction of

13

310   THIARH with O_2 and sequential oxidation initiated by $CO_3^{\cdot-}$ leads to the formation of

311   compound **2**, reaction pathway **j**. THIARM addition of O_2, elimination of superoxide and

312   water addition leads to the formation of 6-chloronicotinaldehyde, reaction pathway **k**.

313   **Scheme 3.** Mechanism for the reaction of THIA with carbonate radical anions. Sulphate

314   radical attack to THIA is also shown. Transients and stable products in brackets are

315   proposed, but not detected.
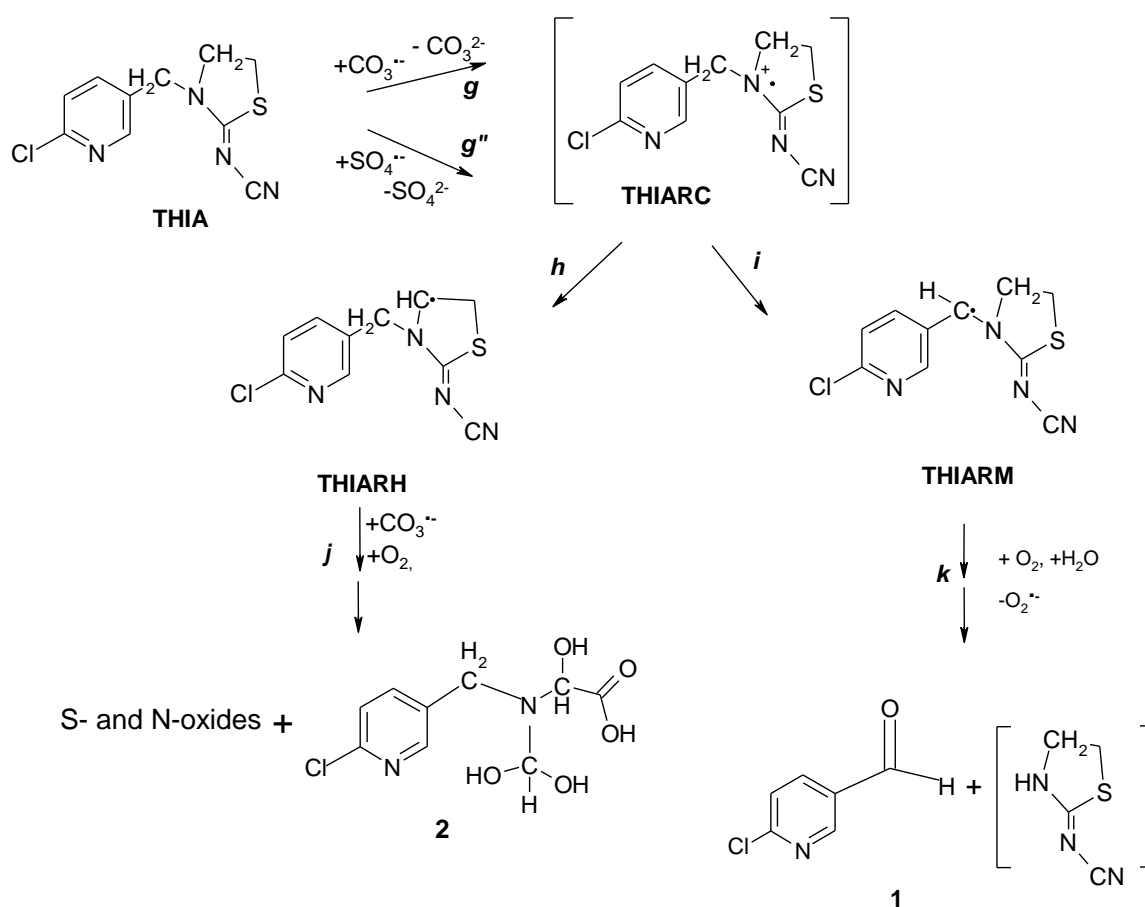
316

317   Formation of products **1** and **3** in experiments with ACT may also be explained by an initial

318   electron transfer pathway from ACT to $CO_3^{\cdot-}$ yielding the radical cation ACTRC and CO_3^{2-}

319   anions (reaction path **l** in Scheme 4), as suggested for IMD and THIA. Further H^+ elimination

320   leads to the formation of α-aminoalkylradicals in the methylene bridge, ACTRM (pathway

14

321   *m*). ACTRM addition of O_2 and water leads to the formation of 6-chloronicotinic aldehyde

322   and the imine product **3**, reaction path ***n***.

323   ***Scheme 4***. Proposed reaction mechanism for the reaction of ACT with carbonate radical

324   anions. Sulphate radical attack to ACT is also shown. Transients and stable compounds in

325   brackets are proposed, but not detected.

326

327
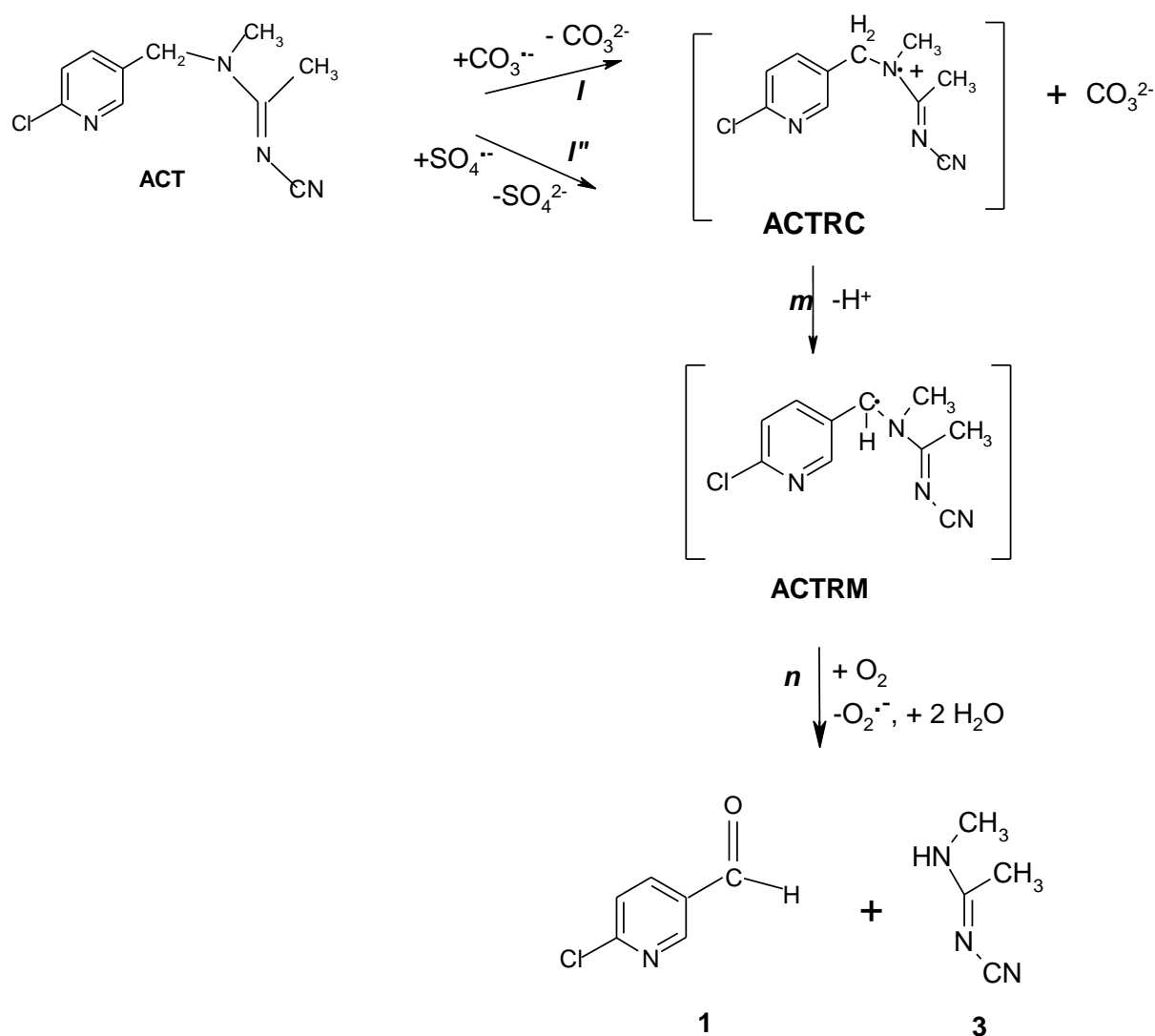
328   The computer simulations shown in Figure 2 predict that only around 40% (30%) of the

329   formed primary products are due to the reaction of ACT (THIA) with $CO_3^{\cdot-}$; the remaining

330   percentage is due to the insecticides reaction with $SO_4^{\cdot-}$ radicals. The reported reaction

331   pathway of $SO_4^{\cdot-}$ radical attack to the insecticides (Dell´Arciprete *et al.*, 2011) is coincident

332   with that proposed here for $CO_3^{\cdot-}$; therefore, the same primary products are formed from

333   reactions (4) and (5), as is the case of products *1* and *3*. Product *2* is formed from the

334   primary products successive oxidation by $CO_3^{\cdot-}$, as they were only observed in experiments

335   in the presence of CO_3^{2-} anions. Therefore, Schemes 3 and 4, also include $SO_4^{\cdot-}$ radical

336   attack to THIA and ACT, reaction paths *g´´* and *l´´*, respectively.

337   **4. *Discussion***

338   Large amounts of the neonicotinoid insecticides reach the natural aqueous systems where

339   they may be degraded by biotic and abiotic pathways. Natural reservoirs show low

340   concentrations of oxidizing radicals (see Table 3), such as hydroxyl ($HO^{\cdot}$) and $CO_3^{\cdot-}$ radicals,

341   singlet oxygen ($^1O_2$), and excited triplet states of dissolved organic matter, ^3DOM, which are

342   capable of initiating the oxidation of the pesticides. To evaluate the detoxifying capacity of

343   natural water towards the different insecticides, a minimum reaction mechanism is

344   considered which consists of the reactions of the insecticides with $CO_3^{\cdot-}$ and $HO^{\cdot}$ radicals,

345    $^1O_2$, and ^3DOM, reactions (4), (9), (10) and (11), respectively, in Table 4. The absorption of

346   355 nm light by DOM produces ^3DOM of 160 kJ mol^{-1} energy (Bruccoleri *et al.*, 1990,

347   Bruccoleri *et al.*, 1990), of the order of Rose Bengal triplet. Therefore, k_{11} is assumed to be

348   of the order of that reported for the reaction of the insecticides with Rose Bengal triplet

349   (Dell´Arciprete et al., 2010). Table 3 shows the steady-state concentrations of reactive

350   oxidants reported for natural waters, also containing dissolved O_2, DOM, carbonates, etc.

351   Scavenging of these oxidants by the natural water matrix components is already accounted

352   for in the reported values. Therefore, the solution of the mass differential equations built for

353   the latter set of reactions considering the steady-state concentrations of the reactive

354   oxidants depicted in Table 3 yields information on the expected lifetime of the insecticides

355   and on the amount of insecticide depleted due to the different reactive intermediates in

356   natural waters. The obtained relations are shown in S.I.6.

16

357   Table 3 about here

358   Table 4 about here

359   An average half life ($t_{1/2}$), as obtained from eq. (5), of 16.0, 4.6 and 4.0 hs is expected for

360   IMD, ACT, and THIA, respectively, under the experimental conditions of a "natural water" of

361   the characteristics described before. Figure 3 shows the predicted depletion of 1×10^{-8} M

362   concentration of each of the insecticides after 16 hours in the "natural water". Singlet

363   molecular oxygen is the most effective species degrading the insecticides, as it is able to

364   degrade 46 % IMD, 81 % THIA, and 86 % ACT. Despite HO$^{\bullet}$ radicals show the smallest

365   steady-state concentration, they are responsible for the depletion of almost 49 % IMD, 16 %

366   THIA, and 13 % ACT. Despite its higher concentration, carbonate radicals is the least

367   effective oxidant in depleting the insecticides.

368

369    $t_{1/2} = \ln2 \, / \, (k_{(CO_3^- + Ins)}\times[CO_3^{\bullet -}]_{ss} + k_{(^1O_2 + Ins)}\times[^1O_2]_{ss} + k_{(HO^\bullet + Ins)}\times[HO^\bullet]_{ss} + k_{(^3DOM + Ins)}\times[^3DOM]_{ss})$

370   eq. (5)

371   Figure 3 about here

372   **5. *Conclusions***

373   The insecticides IMD, THIA, and ACT chemically react with $CO_3^{\bullet -}$ radical anions with rate

374   constants of $(4 \pm 1)\times10^6$, $(2.8 \pm 0.5)\times10^5$, and $(1.5 \pm 1)\times10^5$ M^{-1} s^{-1}, respectively. The amidine

375   nitrogen of the molecule is the preferred site of attack of the insecticides, as also observed

376   for SO$_4^{\bullet -}$ radical, singlet oxygen, and the triplet state of Rose Bengal (Dell´Arciprete *et al.*,

377   2009, 2010 and 2011).

378   The low reactivity observed for $CO_3^{\bullet -}$ compared to HO$^\bullet$ radicals and $^1O_2$ indicates that it is

379   little effective in depleting neonicotinoid insecticides. It would take around 6.6 months and

380   7.4 years to degrade IMD and ACT, respectively, in natural waters containing only $CO_3^{\bullet -}$

381   radicals as scavengers.

17

382 Adequate Advanced Oxidation Processes (AOP) for treatment of water and wastewaters

383 contaminated with IMD, ACT, and THIA should be based on the generation of either $HO^{\bullet}$ or

384 $SO_4^{\bullet-}$ radicals as the main oxidizing species. The presence of CO_3^{2-} / HCO_3^{-} anions in the

385 water matrix will considerably diminish the efficiency of the process.

394 **References**

395 Alegre, M. L., Geronés, M., Rosso, J. A., Bertolotti, S. G., Braun, A. M., Mártire, D. O.,

396 Gonzalez, M. C., 2000. Kinetic study of the reactions of chlorine atoms and $Cl_2^{\bullet-}$ radical

397 anions in aqueous solutions. 1. Reaction with benzene. Journal Physical Chemistry A 104

398 (14), 3117- 3125.

399 Baciocchi, E., Del Giacco, T. Lapi, A., 2004., Oxygenation of benzyldimethylamine by singlet

400 oxygen. Products and Mechanism. Organic Letters 6, 4791-4794.

401 Behar, D., Czapski, G., Duchovny, I., 1970. Carbonate radical in flash photolysis and pulse

402 radiolysis of aqueous carbonate solutions. Journal of Physical Chemistry 74 (10), 2206-

403 2210.

404 Bruccoleri, A., Langford, C.H., Arbour,C., 1990. Pulsed photo acoustic evaluation of

405 intersystem crossing quantum yields in fulvic acid. Environmental Technology Letters 11 (2),

406 169–172.

18

407 Bruccoleri, A., Pant, B., Sharma, D. K., H.Langford, C., 1993. Evaluation of primary

408 photoproduct quantum yields in fulvic acids. Environmental Science and Technology 27 (5),

409 889-894.

410 Busset, C., Mazellier, P., Sarakha, M., De Laat, J., 2007. Photochemical generation of

411 carbonate radicals and their reactivity with phenol. Journal of Photochemistry and

412 Photobiology A 185 (2), 127-132.

413 Canonica, S., Jans, U.,Stemmler, K., Hoigne, J.,1995. Transformation Kinetics of Phenols in

414 Water: Photosensitization by Dissolved Natural Organic Material and Aromatic Ketones.

415 Environmental Science and Technology 29 (7), 1822-1831.

416 Canonica, S., Kohn, T., Mac, M., Real, F.J., Wirz, J., von Gunten, U., 2005. Photosensitizer

417 method to determine rate constants for the reaction of carbonate radical with organic

418 compounds. Environmental Science and Technology 39 (23), 9182-9188.

419 Cernigoj U., Stanga, U.L., Trebse, P., 2007. Degradation of neonicotinoid insecticides by

420 different advanced oxidation processes and studying the effect of ozone on TiO_2

421 photocatalysis. Applied Catalysis B 75 (3), 229-238.

422 Criquet, J., Karpel Vel Leitner, N., 2009. Degradation of acetic acid with sulfate radical

423 generated by persulfate ions photolysis. Chemosphere 77 (2), 194–200.

424 Czapski, G., Holcman, J., Bielski, B.H.J., 1994. Reactivity of Nitric Oxide with Simple Short-

425 Lived Radicals in Aqueous Solutions. Journal of American Chemical Society 116 (25),

426 11465-11469.

427 Dell 'Arciprete, M. L., Cobos, C. J., Furlong, J. P., Mártire, D. O., Gonzalez, M.C., 2007.

428 Reactions of Sulphate Radicals with Substituted Pyridines: A Structure–Reactivity

429 Correlation Analysis. ChemPhysChem 8 (17) 2498- 2505.

430 Dell´Arciprete, M.L., Santos-Juanes, L., Arques Sanz, A., Vicente, R., Amat, A. M., Furlong,

431 J.P., Mártire, D. O., Gonzalez, M. C., 2009. Reactivity of hydroxyl radicals with neonicotinoid

432 insecticides: mechanism and changes in toxicity. Photochemistry and Photobiology Sciences

433 8 (7), 1016-1023.

19

434 Dell´Arciprete, M. L., Santos-Juanes, L., Arques, A., Vercher, R.F., Amat, A. M., Furlong, J.

435 P., Mártire, D. O., Gonzalez, M. C., 2010. Reactivity of neonicotinoids pesticides with singlet

436 oxygen. Catalysis Today 151 (1), 137-142.

437 Dell´Arciprete, M. L., Cobos, C. J., Mártire, D. O., Furlong, J. P., Gonzalez, M. C., 2011.

438 Reaction kinetics and mechanisms of neonicotinoid pesticides with sulphate radicals. New

439 Journal of Chemistry 35 (3), 672–680.

440 Elango, T. P., Ramakrishnan, V., Vancheesan, S., Kuriacose, J. C., 1985. Reaction of the

441 carbonate radical with aliphatic amines. Tetrahedron 41 (18), 3837-3843.

442 Elango, T. P., Ramakrishnan, V., Vancheesan, S., Kuriacose, J. C., 1984. Reaction of the

443 carbonate radical with substituted anilines. Proceedings of the Indian National Science

444 Academy (Chem. Sci.) 93 (1) 47-52.

445 Gear, C.W., 1971. Numerical Initial Value Problems in Ordinary Differential Equations.

446 Prentice – Hall, Englewood Cliffs, New Jersey.

447 Haygarth, K.S., Marin, T.W., Janik, I., Kanjana, K., Stanisky, C.M., Bartels, D.M., 2010

448 Carbonate Radical Formation in Radiolysis of Sodium Carbonate and Bicarbonate Solutions

449 up to 250 °C and the Mechanism of its Second Order Decay. Journal of Physical Chemistry

450 A 114(5), 2142–2150.

451 Herrmann, H., Reese, A., Zelhrer, R., 1995 Time-resolved UV/VIS Diode Array Radical

452 Anions in Aqueous Solution Absorption Spectroscopy of SO_x^-(x=3, 4, 5). Journal of

453 Molecular Structure 348, 183-186.

454 Hiller, K. O., Asmus, K. D., 1983. Formation and reduction reactions of α-amino radicals

455 derived from methionine and its derivatives in aqueous solutions. Journal of Physical.

456 Chemistry 87 (19), 3682–3688.

457 Huang, J., Mabury, S. A., 2000. a) The role of carbonate radical in limiting the persistence of

458 sulfur-containing chemicals in sunlit natural waters. Chemosphere 41 (11), 1775-1782. b) A

459 new method for measuring carbonate radical reactivity toward pesticides. Environmental

460 Toxicology and Chemistry 19 (6), 1501-1507.

461   Lalevée, J., Graff, B., Allonas, X., Fouassier, J. P., 2007. Aminoalkyl Radicals: Direct

462   Observation and Reactivity toward Oxygen, 2,2,6,6-Tetramethylpiperidine-*N*-oxyl, and

463   Methyl Acrylate. Journal of Physical Chemistry A 111 (30), 6991-6998.

464   Lam, M.L., Tantuco, K., Mabury, S.A., 2003. Photofate:a new approach in accounting for

465   thecontribution of indirect photolysis of pesticides and pharmaceuticals in surface water.

466   Environmental Science and Technology 37 (5), 899-907

467   Lower, S. K., 1999. Carbonate equilibria in natural waters. Available on the web at:

468   http://www.chem1.com/acad/webtext/pdf/c3carb.pdf (October 2011)

469   Malato, S., Caceres, J., Aguera, A., Mezcua, M., Hernendo, D., Vial, J., Fernandez-Alba, R.,

470   2001. Degradation of Imidacloprid in Water by Photo-Fenton and TiO_2 Photocatalysis at a

471   Solar Pilot Plant: A Comparative Study. Environmental Science and Technology 35 (21),

472   4359-4365.

473   Mazellier, P., Leroy, E., De Laat, J., Legube, B., 2002. Tranformation of carbendazim

474   induced by the H_2O_2/UV system in the presence of hydrogenocarbonate ions: involvement of

475   the carbonate radical. New Journal of Chemistry 26(12), 1784-1790.

476   Mazellier, P. Busset, C. Delmont, A. De Laat J., 2007. A comparison of fenuron degradation

477   by hydroxyl and carbonate radicals in aqueous solution. Water Research 41(20), 4585 –

478   4594.

479   McElroy, W.J., 1990. Laser photolysis study of the reaction of SO_4^{-} with Cl^- and the

480   subsequent decay of Cl_2^{-} in aqueous solutions. Journal of Physical Chemistry 94 (6), 2435 –

481   2441.

482   Moza, P. N., Hustert, K., Feicht, E., Kettrup, A., 1998. Photolysis of imidacloprid in aqueous

483   solution, Chemosphere 36 (3), 497-502.

484   Neta, P., Huie, R.E., Ross, A.B., 1988. Rate constants for reactions of inorganic radicals in

485   aqueous solution. Journal of Physical Chemistry Reference Data 17(3),1027-1229.

486   Padmaja, S., Neta, P., Huie, R.E., 1993. Rate constants for some reactions of inorganic

487   radicals with inorganic ions. Temperature and solvent dependence., International Journal of

488   Chemical Kinetics 25 (6), 445 – 455.

489 Redlich, D., Shahin, N., Ekici, P., Friess, A., Parlar, H., 2007. Kinetical study of the

490 photoinduced degradation of imidacloprid in aquatic media, Clean 35 (5) 452-458.

491 Ross, A. B., Mallard, W. G., Helman, W. P., Buxton, G. V., Huie, R. E., Neta, P.,1998.

492 NDRL-NIST Solution Kinetics Database, 1998: Ver. 3.0x, Notre Dame Radiation Laboratory,

493 Notre Dame, IN and National Institute of Standards and Technology, Gaithersburg, MD,

494 Available on the web at: http://kinetics.nist.gov/solution/ (March 2008)

495 Shafirovih, V., Dourandin, A., Huang, W., Geacintov, N. E., 2001. The carbonate radical is a

496 site-selective oxidizing agent of guanine in double-stranted oligonucleotides. The Journal of

497 Biological Chemistry 276 (27), 24621-24626.

498 Swancutt, K. L., Dail, M. K., Mezyk, S. P., Ishida, K. P., 2010. Absolute kinetics and reaction

499 efficiencies of hydroxyl-radical-induced degradation of methyl isothiocyanate (MITC) in

500 different quality waters, Chemosphere 81 (3), 339–344.

501 Vione, D., Falletti, G., Maurino, V., Minero, C., Pelizzetti, E., Malandrino, M., Ajassa, R.,

502 Olariu, R., Arsene, C., 2006. Sources and Sinks of Hydroxyl Radicals upon Irradiation of

503 Natural Water Samples. Environmental Science and Technology 40 (12), 3775-3781.

504 Vione, D., Maurino, V., Minero, C., Carlotti, M.E., Chiron, S., Barbati, S., 2009. Modelling the

505 occurrence and reactivity of the carbonate radical in surface freshwater. Comptes Rendus

506 Chimie 12 (8) 865-871.

507 Wamhoff, H., Schneider, V., 1999. Photodegradation of imidacloprid, Journal of Agricultural

508 and Food Chemistry 47 (4), 1730-1734.

509 Wu, C.l., Linden, K.G., 2010. Phototransformation of selected organophosphorus pesticides:

510 Roles of hydroxyl and carbonate radicals. Water Research 44 (12), 3585 -3594.

511 Zabar, R., Dolec, D., Jerman, T., Franko, M., Trebse, P., 2011. Photolytic and photocatalytic

512 degradation of 6-chloronicotinic acid. Chemosphere 2011, doi:10.1016/

513 j.chemosphere.2011.06.107.

514 Zepp, R.G., Wolfe, N. L., Baughman, G.L., Hollis, R.C., 1977. Singlet oxygen in natural

515 waters. Nature 267 (5610), 421-423.

516

Figure Captions:

Fig.1- Absorbance traces at 600 nm obtained in experiments with solutions containing 0.025

M $Na_2S_2O_8$ and 1 M Na_2CO_3 in the presence (grey curve) and absence (black curve) of

1×10^{-5} M of IMD. The dotted grey line stands for the computer simulation obtained for $CO_3^{\bullet-}$

profiles under the experiment conditions in the absence of IMD (see text). The dashed black

line stands for the computer simulation obtained for $CO_3^{\bullet-}$ profiles under the experiment

conditions in the presence of 1×10^{-5} M IMD (see text). *Inset*: Apparent rate constant as a

function of insecticide concentration for (▼) THIA and (●) ACT. The dashed curves show

the confidence interval at 95 %.

Fig. 2 - Transient spectra retrieved by a bilinear analysis of the absorption matrix obtained

from flash photolysis experiments of air saturated solutions containing 0.025M $S_2O_8^{2-}$; 1 M

HCO_3^- and $2x10^{-4}$ M IMD. The solid grey line stands for the spectrum of the $CO_3^{\bullet-}$ radical

obtained in experiments under identical conditions but in the absence of the insecticide. The

dashed grey line stands for the 0.46×IMDRM + 0.54×IMDRH combination of the theoretical

spectrum of IMDRM and IMDRH taken from Dell´Arciprete *et al.*, 2011. *Inset*: Contribution of

$CO_3^{\bullet-}$ radical (curve ***a***) and the organic transient formed after reaction (4) (curve ***b***) to the

absorbance of the traces at 600 and 330 nm, respectively, for the experiments shown in the

main figure.

Fig. 3 - Expected IMD, THIA and ACT degradation after 16 hs in "artificial natural water"

containing 1×10^{-8}M initial concentrations of the insecticide, and steady state concentrations

$[HO^\bullet]_{ss} = 1\times10^{-16}$M, $[^1O_2]_{ss}= 1\times10^{-12}$M, $[CO_3^{\bullet-}]_{ss} = [^3DOM]_{ss} = 1\times10^{-14}$ M. The consumption

due to the different scavengers is depicted as: black: $HO^\bullet$, red: $CO_3^{\bullet-}$(not visible in the scale),

green: ^3DOM and yellow: $^1O_2$,

Table 1 - Manifold of reactions taking place upon UV-light activation of peroxodisulphate in the reaction mixture composed of $S_2O_8^{2-}$, CO_3^{2-}, and the insecticide. The corresponding reaction rate constants k at 25 ^oC are also shown.

Reaction	$k / M^{-1}s^{-1}$	
$S_2O_8^{2-}$ + $h\nu$ → 2 $SO_4^{\bullet-}$	$I_{abs} \times \phi(SO_4^{\bullet-})$ [a]	(1)
$SO_4^{\bullet-}$ + HCO_3^- → SO_4^{2-} + H^+ + $CO_3^{\bullet-}$	4.1×10^6 [b]	(2)
$CO_3^{\bullet-}$ + $CO_3^{\bullet-}$ → $C_2O_6^{2-}$ (+ 2H^+) →→ 2CO_2 + H_2O_2	$(5.5 \pm 0.4)\times10^6$ [c]	(3)
Insecticide + $CO_3^{\bullet-}$ → CO_3^{2-} + Organic radical	$k_{4,IMD} = (4 \pm 2)\times10^6$ [d]	(4)
	$k_{4,ACT} = (1.5 \pm 1)\times10^5$ [d]	
	$k_{4,THIA} = (2.8 \pm 0.5)\times10^5$ [d]	
Insecticide + $SO_4^{\bullet-}$ → SO_4^{2-} + Organic radical	$k_{5,IMD} = (3 \pm 1)\times10^8$ [e]	(5)
	$k_{5,ACT} = (1.1\pm0.6)\times10^9$ [e]	
	$k_{5,THIA} = (3\pm1)\times10^9$ [e]	
$SO_4^{\bullet-}$ + H_2O → SO_4^{2-} + $HO^\bullet$ + H^+	$(6.6 \pm 0.4)\times10^2$ [f]	(6)
$SO_4^{\bullet-}$ + $S_2O_8^{2-}$ → $S_2O_8^{\bullet-}$ + SO_4^{2-}	$(6.3 \pm 1.5)\times10^5$ [f]	(7)
2 $SO_4^{\bullet-}$ → $S_2O_8^{2-}$	5×10^8 [g]	(8)

(a) I_{abs} is the absorbed photonic flux and $\phi(SO_4^{\bullet-})$ is the peroxodisulphate photodissociation quantum yield. (b) Data obtained from Ref. (Padmaja *et al.*, 1993). (c) This work, for ionic strength = 1.08, products from reference (Haygarth *et al.*, 2010). (d) *k* values from this work. (e) Data obtained from Ref. (Dell´Arciprete *et al.*, 2011) (f) Data obtained from Ref. (Herrmann *et al.*, 1995). (g) Data obtained from Ref. (Ross *et al.*, 1998)

Table 2 - Observed degradation products formed after the reaction of $CO_3^{\bullet-}$ radicals with the insecticides, see text. GC retention times, R_t, and MS mass to charge ratios m/z, are given, together with assigned products.

Insecticide	15 minutes irradiation m/z, R_t in min.	30 minutes irradiation m/z, R_t in min	Product assignment
IMD	140, 112, 85, 76 R_t= 11.5		6-chloronicotinic aldehyde, compound **1** in Sch. 2
	264, 153, 126 R_t= 37.5		(N-(1,1-dihydroxy)methyl)-(N-(1-hydroxy,2,2-dihydroxy)ethyl)-2-chloro-5-pyridin-5-ylmethanamine compound **2** in Sch. 2
THIA	140, 112, 85, 76 R_t= 11. 5	140, 112, 85, 76 R_t= 11.5	6-chloronicotinic aldehyde, compound **1**.
	264, 153, 126 R_t= 37.5	264, 153, 126 R_t= 37.5	(N-(1,1-dihydroxy)methyl)-(N-(1-hydroxy,2,2-dihydroxy)ethyl)-2-chloro-5-pyridin-5-ylmethanamine, compound **2**.
ACT	97, 82, 67 R_t = 18.5		N´-cyano-N-methyl acetamidine, compound **3**, Sch. 4.
	140, 112, 85, 76 R_t= 11.5		6-chloronicotinic aldehyde, compound **1**.

Table 3 - Natural water abundance of reactive intermediates and corresponding reaction rate constants k at 25 $^{\circ}$C for IMD, THIA, and ACT.

Reactive Oxidant (RO)	$CO_3^{\bullet-}$ radicals	$^1O_2$	DOM triplet	$HO^{\bullet}$ radicals
Natural water abundance / M	10^{-13}-10^{-15} [a]	10^{-12} - 10^{-13} [b]	10^{-13} - 10^{-15} [c]	10^{-17}-10^{-15} [d]
$k_{(IMD + RO)}$ / $M^{-1}s^{-1}$	$(4 \pm 1) \times 10^{6}$ [e]	$(5.5 \pm 0.5) \times 10^{6}$ [f]	$(4.8 \pm 1) \times 10^{7}$ [g]	6×10^{10} [h]
$k_{(THIA + RO)}$ / $M^{-1}s^{-1}$	$(2.8 \pm 0.5) \times 10^{5}$ [e]	$(3.9 \pm 1) \times 10^{7}$ [f]	$(1.5 \pm 1) \times 10^{8}$ [g]	7.5×10^{10} [h]
$k_{(ACT + RO)}$ / $M^{-1}s^{-1}$	$(1.5 \pm 1) \times 10^{5}$ [e]	$(3.6 \pm 1) \times 10^{7}$ [f]	$(3.6 \pm 1) \times 10^{7}$ [g]	5.5×10^{10} [h]

(a) From ref. (Canonica *et al.*, 2005, Lower, 1999). (b) From ref. (Zepp 1997). (c) From ref. (Canonica *et al.*,1995). (d) From ref. (Vione *et al.*, 2006). (e) This work. (f) From ref. (Dell' Arciprete *et al.*, 2010). (g) From ref. (Dell' Arciprete *et al.*, 2010). (h) Taken from ref. (Dell' Arciprete *et al.*, 2009).

Table 4 - Manifold of reactions depleting the neonicotinoid insecticides in natural waters. The corresponding rate constants at 25 $^{\circ}$C are shown in Table 3. P_i stands for the organic radical of reaction i.
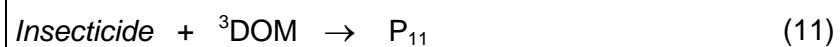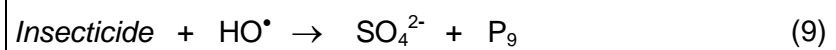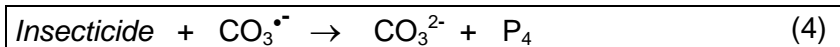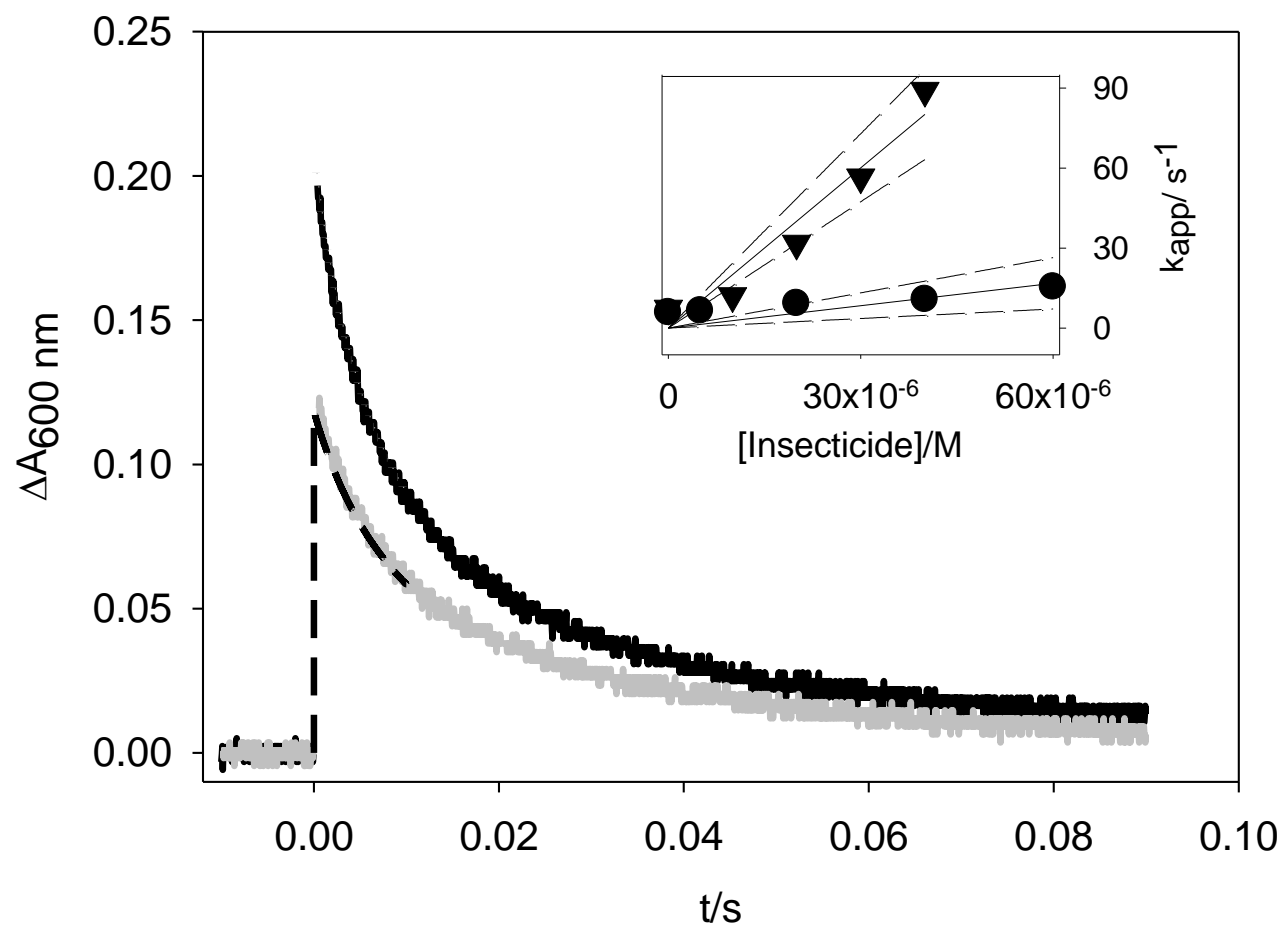
$$
\begin{array}{lll}
\textit{Insecticide} + CO_3^{\bullet-} \rightarrow CO_3^{2-} + P_4 & & (4) \\
\textit{Insecticide} + HO^{\bullet} \rightarrow SO_4^{2-} + P_9 & & (9) \\
\textit{Insecticide} + {}^{1}O_2 \rightarrow P_{10} & & (10) \\
\textit{Insecticide} + {}^{3}DOM \rightarrow P_{11} & & (11)
\end{array}
$$
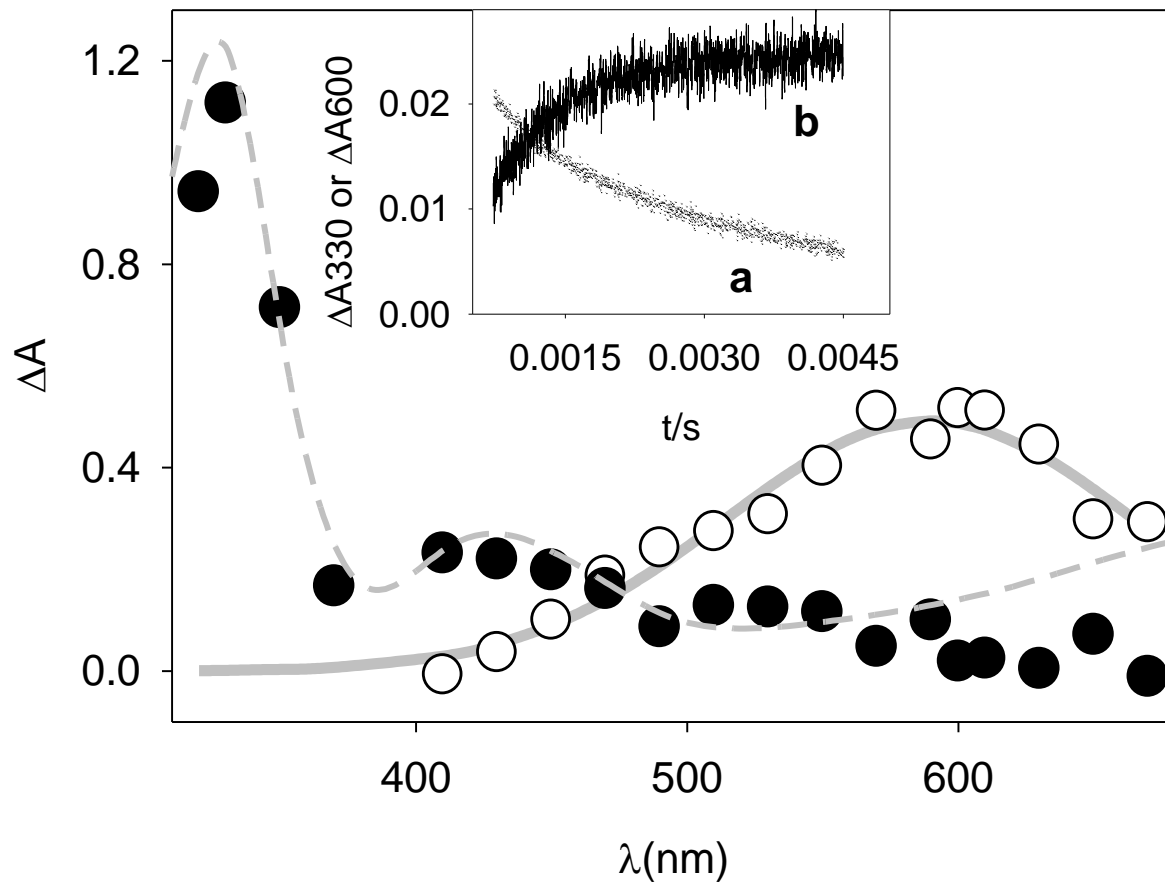
Figure 1

Figure 2

Figure 3
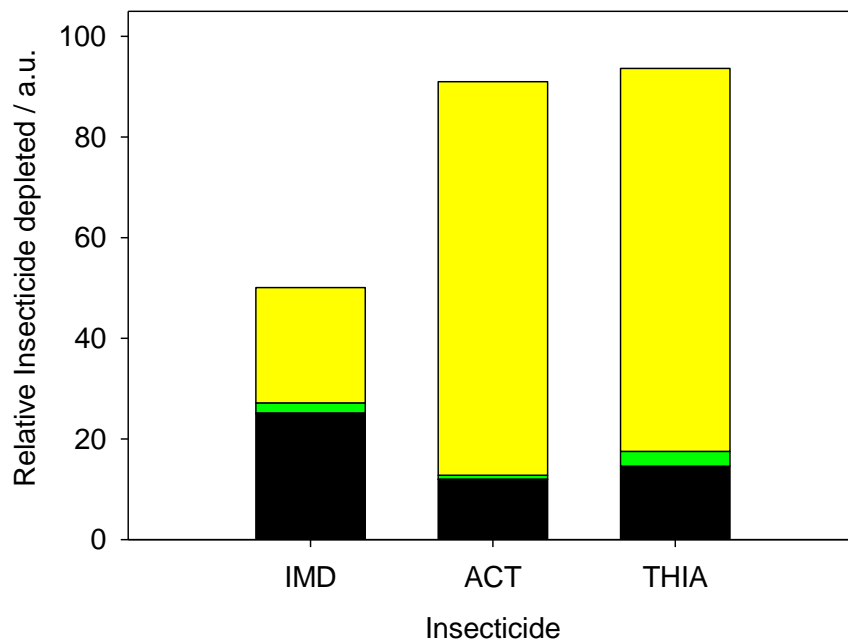
Electronic Supplementary Material (for online publication only)